

Subsurface Diagnosis With Time-Lapse GPR Slices and Change Detection Algorithms

Tess Xiang-Huan Luo  and Wallace Wai Lok Lai 

Abstract—This article explores the capability of applying time-lapse ground penetrating radar (GPR) data to investigate the health condition of an urban subsurface. A workflow is proposed to semi-automatically extract changes from time-lapse GPR C-scans. The developed workflow consists of two main steps, in which the first step is image registration and intensity normalization. The workflow uses benchmark points on the ground to normalize the global intensity of time-lapse GPR C-scans. The second step classifies pixels into change or unchanged group. Two kinds of information are considered to construct two difference-maps: changes in the image intensity and the object structure. K-means clustering is responsible for extracting pixels that possess both intensity changes and object structure changes – where potential subsurface defects most likely occurred. The workflow was verified by a site experiment, and the area of excavation with pipe replacement was successfully identified. The performance of the proposed workflow was promising in excluding small and random scattering noise, which was the main challenge in a time-lapse GPR survey. The article serves as a prototype and demonstrates the feasibility and necessity of conducting temporal diagnosis on the subsurface structure.

Index Terms—Ground penetrating radar (GPR), subsurface diagnosis, temporal change detection, time-lapse.

I. INTRODUCTION

MODERN cities are facilitated by a large number of underground utilities. However, the management of these subsurface infrastructures is complicated, and the work of managing invisible underground utilities has proven to be especially demanding and costly. Without proper diagnosis and maintenance, ageing utilities can suffer from various modes of failures, bringing urban hazards such as land subsidence, the collapse of infrastructure, and flooding. They can cause not only financial loss, but also causalities. Conducting regular health checks for

condition diagnosis on urban underground utilities is a relatively novel approach. A ground penetrating radar (GPR) is one of the most suitable means for imaging the subsurface. The GPR makes the use of the transmission and reflection of the electromagnetic wave to detect dielectric properties change in host materials [2], [3]. The C-scan (depth/time slice) is a three-dimensional (3-D) representation of the GPR data that can provide straightforward images on the subsurface.

Due to the complex and unknown environment of subsurface, biases from human perception are inevitable in generating GPR C-scans. It is suggested that a single measurement is not reliable enough for determining small changes. Establishing a “medical record” with a series of time-lapse GPR C-scans is a way to extract potential subsurface defects. Besides, if we have a baseline depicting how a healthy situation should present in GPR data, then by comparing this baseline with images obtained later, potential defects can be relatively easily located from GPR C-scans by techniques of change detection from images. This approach further facilitates the possibility of conducting subsurface surveys that have a city-scale coverage: if only changed areas need to be inspected, the workload will be decreased significantly. A fast and robust method for change-detection from images is desired to extract dissimilarities among time-lapse GPR C-scans for further investigation.

Appropriate customization is essential when adapting image change detection techniques to GPR C-scans. A successful implementation was provided by Hong *et al.* [4], which detected corrosion in reinforced concrete using the intensity change in GPR C-scans. Temporal changes in GPR data are affected by various factors including moisture conditions, temperature, and equipment spectral range. Given that the resolution of GPR images can go up to centimeters, the mathematical pixel-based method may be ineffective in that range. However, object edges in GPR images are not sharply depicted because of the polarity of the material, which makes it difficult to extract the correct object with the object-based methods of a change detection. The information available in GPR C-scans is too limited – only reflection intensity is described in GPR C-scans, it may be insufficient for supervised change detection methods. In summary, the unsupervised pixel-based change detection method is the most suitable approach for temporal GPR C-scans. This article explores the feasibility of applying unsupervised method for change detection from images, to semi-automatically identify subsurface defects from time-lapse GPR C-scans. A workflow that integrates K-means clustering is proposed and validated with a case study.

Manuscript received October 10, 2019; revised January 26, 2020; accepted February 15, 2020. Date of publication February 28, 2020; date of current version March 17, 2020. This work was supported in part by the Research Institute for Sustainable Urban Development, the Hong Kong Polytechnic University, under Grant PolyU 1-BBWB (Development of a Strategic Focus Area (SFA) in Utility System Research) and in part by the Grant PolyU 152648/16E (A study of water seepage in construction materials with phase velocity dispersion of wide-band ground penetrating radar wave and spectral analysis of surface wave). (Corresponding author: Wallace Wai Lok Lai.)

Tess Xiang-Huan Luo is with the Department of Land Surveying and Geo-Informatics, Hong Kong Polytechnic University, Hong Kong (e-mail: tess.luo@connect.polyu.hk).

Wallace Wai Lok Lai is with the Department of Land Surveying and Geo-Informatics, Hong Kong Polytechnic University, Hong Kong and also with Research Institute for Sustainable Urban Development, The Hong Kong Polytechnic University, Hung Hom, Hong Kong (e-mail: wllai@polyu.edu.hk).

Digital Object Identifier 10.1109/JSTARS.2020.2975659

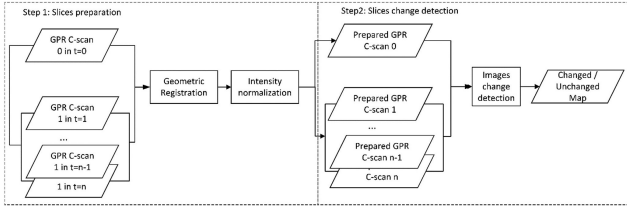


Fig. 1. General workflow of temporal changes extraction from time-lapse GPR C-scans.

II. WORKFLOW OF TEMPORAL CHANGES EXTRACTION FROM TIME-LAPSE GPR C-SCANS

Given the complexity of GPR C-scans, a standardized 3-D imaging workflow is required to make sure the time-lapse GPR C-scans are reliable for comparison, with as little as possible human judgments introduced [5]. The GPR C-scans are semantic images that variations among time-lapse C-scans are inevitable. Proper pre-processing for reducing the subjective discrepancies among time-lapse C-scans is the key to success in changes detection. A workflow that integrates imaging pre-processing and image change detection technique is proposed in this article. The workflow consists of two stages: image preparation and changes detection, as shown in Fig. 1.

A. GPR C-Scans Geometric and Intensity Rectification

The GPR C-scan images are that generated by similar criteria can be used for change detection. The reflection intensity and positions of the two images must be consistent [6]. Such that corresponding geo-referenced pixels in an image should describe the reflection of the same position. The pixel values, which depicting the reflection intensity of the same position, should be within the same color coding scale. Hence, the first step is the image preparation: register the pixel position and normalize the reflection intensity of the temporal GPR C-scan pair.

For the gridding of GPR survey, positioning errors are mainly caused by the offset between the GPR antenna and the pre-designed grid. Then, the actual GPR traverse grid may not coincide with the recorded grid. Thanks to the integration of a global positioning system and auto-track total station with a GPR system, under certain circumstance, a GPR survey no longer need to follow a predefined grid. But the real-time global positioning itself has errors.

When constructing GPR C-scans, recorded reflection intensities within the system's dynamic range (32, 64 bits) are transformed into digital values of pixels. Applying adjustment on this transform scale could result in different imaging results. Besides, the GPR signals attenuate with increasing depth of penetration. A time-vary gain is always applied to artificially enhance the signal strength in the deeper area to make the GPR reflection "visible." However, the gain function is case-specific as the attenuation rate is determined by the dielectric properties and the conductivity of the host material. The variation in the GPR C-scans process may bring artificial discrepancies into the time-lapse dataset. Therefore, proper amplitude or reflection intensity normalization is required to ensure the pixel values of time-lapse

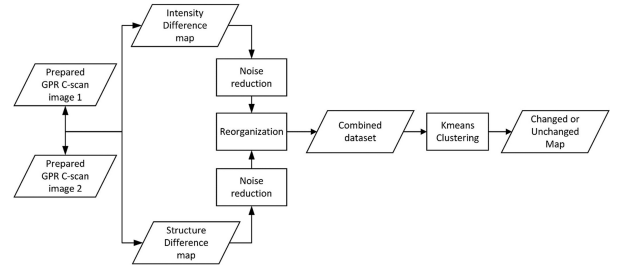


Fig. 2. Workflow of changes detection from two GPR C-scan images.

images are correlated. When C-scans are prepared, they can serve as the input to extract the changes happened underneath the surface.

B. GPR C-Scans Change Detection With K-Means Clustering

Due to lacking of ground truth data, the approach of unsupervised change detection is preferred in time-lapse GPR surveys. Zheng *et al.*, [7] developed a simple and effective method for obtaining a difference from images of temporal-sequential synthetic aperture radar (SAR): the method combined difference images and K-means clustering to classify pixels into the changed or unchanged group. The challenges of detecting temporal changes from GPR C-scan images and SAR images are similar: unknown speckle noises in images makes the change detection much more difficult than that of optical images. The method developed by Zheng *et al.* [7] was adopted and adapted in this study.

In view of the nature of GPR C-scans – a lot of isolated reflections from clusters are recorded in images; the speckle-noise reduction is very important for the entire process. The GPR C-scans deliver mainly two kinds of information: one is the reflection intensity, which is shown as pixel values; another is the object structure – including object shape, size, manifested as either a continuous object or a local object. This article makes the use of these two kinds of information to distinguish changed areas from the unchanged ones. Therefore, the change detection method adopted in this article mainly composes of three steps: 1) produce maps of difference – a reflectance's change map and a structure's change map; 2) noise reduction by filtering – remove random scatterings; and 3) label the changed area by K-means clustering. The general workflow of the change detection is shown in Fig. 2.

Among many unsupervised methods, K-means is selected because it is a simple but mature algorithm: it partitions data into K clusters by repeatedly minimizing the within-cluster sum of squares. Originally proposed by MacQueen [8], the general description of the K-means clustering method is given as

$$\arg \min_S \sum_{i=1}^k \sum_{x \in S_i} \|x - \mu_i\|^2 = \arg \min_S \sum_{i=1}^k |S_i| \text{Var} S_i \quad (1)$$

where μ_{i_i} is the mean of points in data S_i .

The algorithm starts with a random seed, and then, partition the data into clusters with the Voronoi diagram: assign the data point to a cluster whose mean has the least squared Euclidean

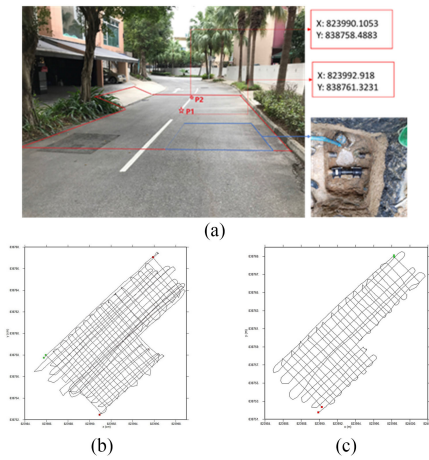


Fig. 3. Illustration of the site area and survey paths. (a) Photo of the case site: A piece of road in the Royal Palm. (b) and (c) Survey paths tracked by the total station in the first and the second survey, respectively. The survey paths were approximately orthogonal grid, and green and red dots refer to the start point and the end point, respectively.

distance. Afterwards, the centroid of each cluster is calculated. The algorithm repeats the process at another random seed until the sum distance of all data points to their cluster centroid is the minimum. The algorithm does not guarantee the optimum [9], [10]. The proposed method is computationally efficient and requires limit ground truth information, which makes it suitable for working on low dimension GPR C-scans.

III. WORKFLOW VALIDATION WITH A SITE EXPERIMENT

A. Site Specification

A case study was conducted in the Royal Palm to verify the proposed workflow. The Royal Palm is a large private residential area in Hong Kong. There are sophisticated underground utilities buried underneath. If a utility bursts, residents' daily life would be affected seriously.

A section of the bituminous road in the Royal Palm is taken as a case (see Fig. 3) to illustrate the feasibility of temporal observation with GPR. This section of the road was determined as old with needs of repair or replacement. Two GPR surveys were conducted at different times: the first survey served as the baseline survey, and then, an excavation was undertaken for the utility maintenance and serves as ground truth as well. The excavation area was 1.5×2 m large and 1.5 m deep, as shown in Fig. 3(a). Then, after backfilling the evacuation area with the soil dugout, the second GPR survey was carried out a week later with the same survey setting as that of the first survey.

B. Survey Specification

During the two surveys, two points were selected as benchmarks for adjusting the reflection intensity of the GPR data. The two points located within the survey area but were far away from the excavation site. GPR reflection intensities at these two points were supposed to be very similar.

The GPR data were collected by an IDS 200/600 MHz dual frequency system equipped with an auto-track total station.

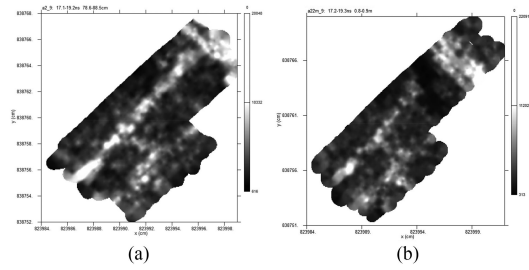


Fig. 4. GPR C-scans of the two surveys at 0.85-m depth. (a) First survey. (b) Second survey.

Every single trace (A-scan) was related to coordinates measurements in the HK-80 projection coordinate system.

Underground utilities are normally buried within a few metres deep; thus, in this case, only the 600 MHz data were investigated. The center frequency of GPR data collected by 600 MHz antenna was measured as 514 MHz with the wavelet transform [11]

IV. EXPERIMENT RESULTS AND ANALYSIS

A. Image Preparation Result

Standard signal processing, including de-wow, time-vary gain, frequency domain bandpass filtering, time-zero correction, velocity estimation, and migration were applied with Reflexw on both GPR dataset [3], [12]. The C-scan images were produced with GPR-SLICE from the processed radargram follow a standard 3-D imaging workflow. The 3-D imaging workflow consists of two major steps: vertical slicing and the horizontal interpolation [5]. Since the two surveys were conducted with the same set of equipment, the criteria for both the radargram processing and the C-scan generation were maintained as much similar as possible. The produced C-scans at the utility depth (0.85 m) of two surveys are shown in Fig. 4. A connected higher reflection region can be clearly seen, and it is defined as a water pipe because of its linear connectivity. Both images are speckle with blurry scatterings surrounding the utilities. The reflection intensity at the pipe depth of the first survey was digitized between 616 and 20 048; while that of the second survey was in a similar yet slightly different dynamic range, which was between 313 and 20 091. Even though the processing procedures were almost the same, many discrepancies exist between the temporal GPR C-scans. These discrepancies may be raised by variations in either electronic or slight changes of electrical properties of the host materials.

The auto-track positioning system has been proven effective and efficient in many practices [13], [14]. But the latency between the actual scan position and the measured position is unavoidable, due to the clock error between the GPR clock time and the total station's clock time. Since the latency happened along the survey path, and survey paths of the time-lapse dataset were not coincided [see Fig. 3(b) and (c)], obvious misalignments were observed in the time-lapse dataset. Because the image change-detection requires fully co-registration, which depends on correct positioning, the latency correction was introduced in this study.

As shown in Fig. 4, without latency correction, the utilities are presented as a zig-zag shape, although utilities are made straight

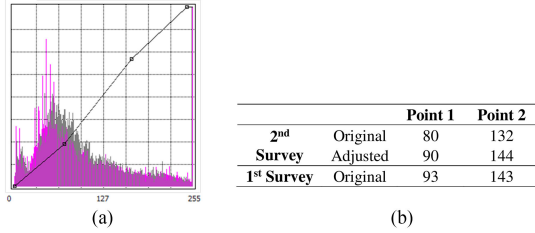


Fig. 5. Adjust the histogram of GPR slice of the second survey to align with that of the first survey.

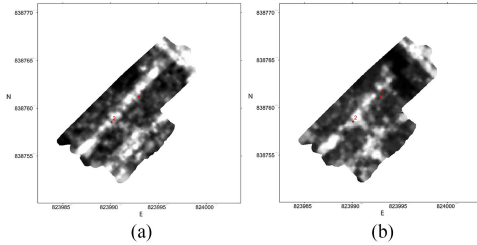


Fig. 6. GPR C-scans with positioning and reflectance strength corrected for two surveys. (a) First survey. (b) Second survey.

certainly. Along the survey path, the offset was calculated from the distance of the peak of zigzag to its center: it was 0.1 m and 0.14 m in two surveys. Given that the two surveys both used 220 scans/m, the latency was estimated as the radargram went 20- and 30-scan faster than the positioning measurement in the first survey and the second survey, respectively. Each GPR trace was shifted along the survey path.

Another essential step in preparing images is correlating the reflection intensities of the two GPR C-scans. As it rained before the second survey, the moisture content of the soils was higher as expected. So it was not surprising that the global reflection intensities between these two surveys were different even though a constant gain was applied. In this article, the emphasis is laid on detecting the changes of utility groups, so the global reflection intensity change was normalized by adjusting the histograms of the two GPR C-scans. The process of intensity normalization was as follow: 1) project the reflection intensity to 8-bit grey value; 2) identify the digital values of the pixels at benchmark points; 3) align the histogram of the second survey with the first survey base on these two benchmark points, as these two benchmark points were supposed to generate a similar GPR reflection intensity. After the amplitude adjustment, the discrepancies of pixel values at benchmark points of two surveys were reduced, as shown in Fig. 5. The common area that two surveys cover was extracted, and this pair of C-scans was ready for further change detection (see Fig. 6).

B. Change Extraction Result

The process of change extraction was accomplished with MATLAB. The very first step was to produce maps of difference. Reflectance intensity's map of difference was produced by a subtracting operator, given in (2), while the difference map of structure was produced by a log-ratio operator, given in (3). The log ratio can smoothen changes in pixels with a larger pixel value

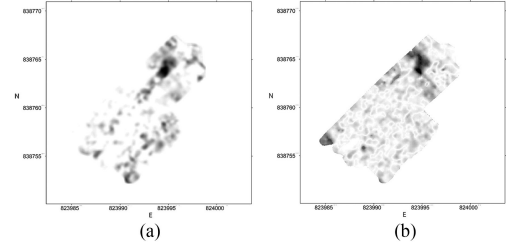


Fig. 7. Difference map (a) is the map shows the intensity difference; (b) shows the structure difference of two GPR depth slice.

but enlarge tiny changes in pixel value smaller than 10. In this way, the edges of objects were enhanced as

$$\text{Intensity difference} = |S_1 - S_2| \quad (2)$$

$$\text{Structural difference} = \left| \log \frac{S_1 + 1}{S_2 + 1} \right| \quad (3)$$

where S_1 and S_2 are pixel values of the first and second GPR depth slice, respectively.

Fig. 7 shows the result of the difference maps. There are dark boundaries surround the survey site, it is mainly due to the image positioning registration error. It further illustrates the importance of precise positioning registration in change detection from images, especially from a very high-resolution GPR image. Both maps of difference compose of a lot of speckle of unwanted scattering of Mie type that the wavelength is comparable to the object size or grain size of soil. Hence, filters were applied to eliminate these noises and reduce the interference information.

A mean filter with an 11×11 structure element was applied on the intensity difference map, while a median filter with a 3×3 structure element was used to smoothen the structure difference map. The structure element for the mean filter was larger so as to remove small and isolate differences, while comparatively a smaller structure element for the difference map of structure can preserve the edge information. Such arrangement emphasized the advantages of each difference map while reducing the bias information. The pixel values of two difference maps were normalized to 8bit, in order to lay equivalent weight on two kinds of information – reflectance and structure. Fake boundaries generated by mis-registration were removed. Both difference maps still possess a large number of “false alarms,” a significant discrepancy was highlighted as dark at the coordinate (823994E, 838763N) in both maps.

The pixel values of two filtered maps were re-organized to construct a two-dimensional dataset for further K-means clustering. Two kinds of information were considered having the same importance in this article. The pixels were to be classified as changed or unchanged, thus the K was two in this study. Meanwhile, the pixel values of two filtered maps were added together to construct a combined map, and the combined map was normalized to 8-bit as well, as shown in Fig. 8. Therefore, the higher pixels value in the change map refers to areas that have more significant changes. The darkest area denotes the place that has the most remarkable changes: replaced pipe. The area labeled as change served as a mask: values of the combined map in this area were assigned to this mask, and the white areas

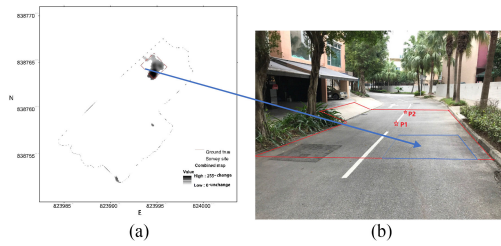


Fig. 8. Temporal changed map that shows the detected evacuation area in the survey site.

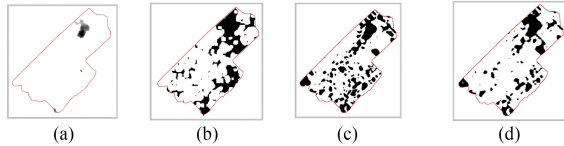


Fig. 9. Comparison of different change detection methods. Results of the (a) proposed method, (b) EM auto-thresholding, (c) PCA, and (d) MRF.

are areas labeled as unchanged. Small and isolate discrepancies were excluded successfully.

V. DISCUSSION ON THE SITE EXPERIMENT

The proposed temporal change detection method was proved to function well in the site experiment. Both feasibilities and challenges were observed during the experiment.

A. Performance of the Proposed Change Detection Method

The detection result was evaluated by comparing with the ground truth – the excavation area. Although there were two small areas [bottom of Fig. 8(a)] wrongly labeled as changed, the majority were correctly classified. Since the proposed unsupervised method required no preliminary knowledge of the subsurface environment, it is particularly suitable for complex subsurface imaging. Furthermore, there was no human interaction included in the whole process, and subjective human error can be avoided.

A comparison of the proposed method with other unsupervised change-detection methods that are widely acknowledged is given in Fig. 9. These methods were Otsu’s auto-thresholding; Principal component analysis (PCA); and Markov random field (MRF) [15]–[17]: they were proved effective in change detection from noises and speckle images. The change detection method proposed in this study performed better, as much less “false alarms” was produced.

The peak signal-to-noise ratio (PSNR) was applied to evaluate the performance of the proposed method. Clustering accuracy was calculated with (4). The proposed method performs better than the others in terms of signal PSNR as well as accuracy as

$$\text{Accuracy} = \frac{TP}{(TP + FP)} \times 100\%. \quad (4)$$

Specifically, Table I also illustrates that the proposed method has less false positives (FPs) compared with other methods. Even though more changed areas were missed (false negative – FN) with the proposed method, the position of the changed area

TABLE I
COMPARISON OF THE PERFORMANCE OF A FEW METHODS

Method	FP	TP	FN	PSNR	Accuracy
Proposed Method	958	3486	1997	20.2542	78%
Otsu EM (Melgani et al., 2002)	23158	5132	351	10.0914	18.14%
PCA (Celik, 2009)	25354	4372	636	9.2956	14.71%
MRF (Wang, 2012)	17165	4669	814	10.9387	21.38%

was precisely located. The comparison Table I shows that the proposed method provided higher PSNR – larger similarity with the ground truth, and the detection accuracy was much higher than other methods. With only reflectance strength presented, GPR C-scans were not informative enough to distinguish actual changes from random small discrepancies. The proposed method solved this problem by assigning meanings – either intensity or structure – to each pixel. It was believed that the clustering methods performed similar, but the construction of difference maps contributed a lot to noise reduction and information extraction and illustrated the importance of preprocessing in the change-detection from GPR C-scans.

B. Preliminary Diagnosis and Locating Potential Defects

The process of change detection from time-series C-scans is the first examination of a diagnosis: similar as seeing a doctor, very often the patients are requested to take medical scans to check whether there is an unusual pattern. If anomalies are noticed, further investigations that are more specific will be conducted before a diagnosis can be given. Usually, the first medical scan does not necessarily give enough details on the course or status of the anomaly. The method proposed in this study can locate changes from GPR C-scans with a few seconds, and the preliminary knowledge about the anomaly, i.e., size and position, can be obtained. Afterwards, more investigation should be conducted on the detected locations: for instance, referring to radargrams or carrying out inversions.

This study illustrates the necessity of conducting temporal GPR surveys for subsurface diagnosis, therefore a practical workflow of time-lapse surveys is proposed. The first step is comparing two C-scans – either a C-scan pair of t_0 , and t_{n-1} , or a C-scans pair of t_{n-1} , and unchanged, then major dissimilarities that indicate potential defects can be identified and extracted. If there is no significant change that means the survey area is healthy and safe. The second step is verifying the detection result with relevant personnel: whether any construction work conducted in this area before. If yes, the change detection result is likely to be TP. Otherwise, further investigation should be implemented. In this way, the condition of the subsurface is tracked continually, and a “medical record” can be built along time. In conclusion, change detection from C-scans can narrow down the areas to be investigated and further facilitate the efficiency of subsurface diagnosis.

C. Improve the Reliability of Time-Lapse C-Scans

Even though with the standardized workflow [5], and the subsurface is correctly imaged, the variations among temporal

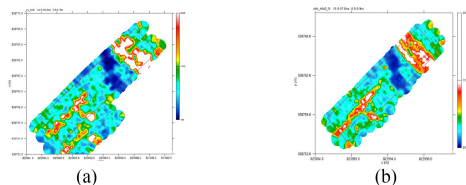


Fig. 10. Comparison of C-scans of surveys without (a) or with (b) the guiding system [1].

GPR C-scans are still inevitable (see Fig. 6). Apart from the variation of the properties of the host material, the variation among time-lapse C-scans is mainly caused by the fact that survey paths of every survey are very different (see Fig. 3) – which is always the case in real practices. Therefore, the survey orientation of a measurement point may vary among surveys of different times, and the polarization of the GPR signal changes accordingly. Moreover, the density of GPR measurements of the 2nd survey was much lower. The denser the GPR measurements, the closer the C-scan to the reality. The lower sample density in the 2nd survey introduced more artificial interpretation in the interpolation step. The blank area among measurements is filled up by interpolation, and interpolation aggravates the discrepancy caused by different survey paths: if there is a contrast between true measurements of different survey times, the calculated measurements are unlikely to coincide, therefore, discrepancies are introduced into blank areas.

Ching [1] developed a guiding system that can guide the GPR operators to walk along a pre-defined grid. As shown in Fig. 10, with the guiding system, the scan lag can be eliminated to a certain degree. In short, in temporal change detection, it is of vital importance to minimize the random variations among time-lapse C-scans.

VI. CONCLUSION

This article explores the capability of applying time-lapse GPR data to investigate the health condition of urban subsurface. A workflow that integrates K-means clustering is proposed to semi-automatically extract changes from time-lapse GPR C-scans. The workflow was verified using a real case study, and the result was promising that the area of excavation was successfully identified while small and random scattering noise. A practical workflow for temporal GPR survey can be concluded from this study. It is suggested to improve the reliability of time-lapse C-scans with coinciding survey paths. The article serves as a prototype and demonstrates the feasibility of conducting temporal diagnosis on the subsurface structure.

ACKNOWLEDGMENT

The authors would like to thank R. Chang, Peter, G. Ching, and S. Yu, for their efforts in collecting GPR data for this article.

REFERENCES

[1] G. P. H. Ching, “Development and validation of a ground penetrating radar (GPR) virtual guiding system for subsurface 3d imaging,” BSc of Geomatics, Dept. Land Surveying and Geo-informatics, The Hong Kong Polytechnic University, 2019.

- [2] A. P. Annan, “GPR—History, trends, and future developments,” *Subsurface Sens. Technol. Appl.*, vol. 3, no. 4, pp. 253–270, 2002.
- [3] H. M. Jol, *Ground Penetrating Radar Theory and Applications*. Oxford, U. K.: Elsevier, 2009.
- [4] S. Hong, H. Wiggerhauser, R. Helmerich, B. Dong, P. Dong, and F. Xing, “Long-term monitoring of reinforcement corrosion in concrete using ground penetrating radar,” *Corrosion Sci.*, vol. 114, pp. 123–132, 2017.
- [5] T. X. Luo, W. W. Lai, R. K. Chang, and D. Goodman, “GPR imaging criteria,” *J. Appl. Geophys.*, vol. 165, pp. 37–48, 2019.
- [6] J. R. Townshend, C. O. Justice, C. Gurney, and J. McManus, “The impact of misregistration on change detection,” *IEEE Trans. Geosci. Remote Sens.*, vol. 30, no. 5, pp. 1054–1060, Sep. 1992.
- [7] Y. Zheng, X. Zhang, B. Hou, and G. Liu, “Using combined difference image and k-means clustering for SAR image change detection,” *IEEE Geosci. Remote Sens. Lett.*, vol. 11, no. 3, pp. 691–695, Mar. 2014.
- [8] J. MacQueen, “Some methods for classification and analysis of multivariate observations,” in *Proc. 5th Berkeley Symp. Math. Statist. Probability*, 1967, vol. 1, pp. 281–297.
- [9] D. J. MacKay, *Information Theory, Inference and Learning Algorithms*. Cambridge, U. K.: Cambridge Univ. Press, 2003.
- [10] E. W. Forgy, “Cluster analysis of multivariate data: Efficiency versus interpretability of classifications,” *Biometrics*, vol. 21, pp. 768–769, 1965.
- [11] W.-L. W. Lai, T. Kind, S. Kruschwitz, J. Wöstmann, and H. Wiggerhauser, “Spectral absorption of spatial and temporal ground penetrating radar signals by water in construction materials,” *NDT E Int.*, vol. 67, pp. 55–63, 2014.
- [12] J. F. C. Sham and W. W. L. Lai, “Development of a new algorithm for accurate estimation of GPR’s wave propagation velocity by common-offset survey method,” *NDT E Int.*, vol. 83, pp. 104–113, 2016.
- [13] K. W. R. Chang, “Real-time tracking and error analysis of ground penetrating radar position by auto-tracking total station,” M.Sc. thesis, Dept. Land Surveying and Geo-informatics, The Hong Kong Polytechnic Univ., Hong Kong, 2016.
- [14] W. W.-L. Lai, X. Dérobert, and P. Annan, “A review of ground penetrating radar application in civil engineering: A 30-year journey from locating and testing to imaging and diagnosis,” *NDT E Int.*, vol. 96, pp. 58–78, 2018.
- [15] T. Celik, “Unsupervised change detection in satellite images using principal component analysis and k-means clustering,” *IEEE Geosci. Remote Sens. Lett.*, vol. 6, no. 4, pp. 772–776, Oct. 2009.
- [16] F. Melgani, G. Moser, and S. B. Serpico, “Unsupervised change-detection methods for remote-sensing images,” *Opt. Eng.*, vol. 41, no. 12, pp. 3288–3298, 2002.
- [17] Q. Wang, “HMRF-EM-image: Implementation of the hidden Markov random field model and its expectation-maximization algorithm,” 2012, *arXiv:1207.3510*.



Tess Xiang-Huan Luo received the M.Sc. degree from the ITC-University of Twente, Enschede, the Netherlands, in 2016. She is currently working toward the Ph.D. degree with the Department of Land Surveying and Geo-Informatics, Hong Kong Polytechnic University, Hong Kong.

Her main research interests include imaging and diagnoses the subsurface defects with ground penetrating radar.



Wallace Wai Lok Lai is currently working as an Associate Professor with the Department of Land Surveying and Geo-Informatics, Hong Kong Polytechnic University, Hong Kong. His main research interests include survey and mapping, 3-D imaging, and diagnosis of engineering structures, underground utilities, and construction materials.